



# Probing the Development of Galaxy Clusters in X rays

A. Cavaliere<sup>1</sup>, R. Fusco-Femiano<sup>2</sup>, and A. Lapi<sup>1,3</sup>

<sup>1</sup> Dip. Fisica, Univ. 'Tor Vergata', Via Ricerca Scientifica 1, 00133 Roma, Italy.

<sup>2</sup> INAF-IASF, Via Fosso del Cavaliere, 00133 Roma, Italy

<sup>3</sup> SISSA, Via Bonomea 265, 34136 Trieste, Italy.

**Abstract.** The development of galaxy clusters is discussed basing on our Supermodel, that expresses in full the entropy-modulated, hydrostatic equilibrium of the intracluster plasma in the DM gravitational wells. We relate central entropy levels to energy injections by AGNs or deep mergers, and the outer entropy distribution to the accretion rates of DM and shocked intergalactic gas. We propose these to decline because of the cosmological slowdown in the outskirts growth at late cosmic times. Thus in addition to explaining the CC vs. NCC cores, we propose conditions leading to steep vs. shallow outer temperature declines, and outline related prospects for WFXT and IXO.

**Key words.** galaxies: clusters: general — X-rays: galaxies: clusters — methods: analytical.

## 1. Introduction

Galaxy clusters with their overall masses up to  $M \sim 10^{15} M_{\odot}$  constitute the largest bound structures in the Universe. Their outskirts extend out to sizes  $R \sim$  a few Mpc, setting the *interface* between the intergalactic environment keyed to the cosmology at large, and the intracluster plasma (ICP; see Cavaliere et al. 2009, hereafter CLFF09). The ICP coexists with the gravitationally dominant dark matter (DM) halo in the baryonic fraction  $m/M \sim 1/6$ , and the two build up together from accretion across the cluster boundary.

In fact, the cluster buildup takes place in two stages; after an early collapse of the DM and gas to set the cluster body, a secular inside-out development of the outskirts follows (see

Zhao et al. 2003; Diemand et al. 2007; Navarro et al. 2010). The body ranges out to radii comparable with  $r_{-2}$  where the slope of the DM density distribution equals  $-2$ ; the adjoining outskirts extend out to the current virial radius  $R$ .

After the transition redshift  $z_t$ , secular accretion begins; then  $r_{-2}$  stays put while  $R$  grows larger in a quasi-static DM equilibrium (that may be described via the Jeans equation, see Lapi & Cavaliere 2009a). This implies for the concentration parameter  $c \equiv R/r_{-2}$  present values  $c \approx 3.5 H(z_t)/H(z_{\text{obs}}) \approx (1 + z_t)/(1 + z_{\text{obs}})$ ; these range from 3 to 10, and correspond to *young* or to *old* cluster ages marked by  $z_t \sim 0.2 - 3$ . The concentration can be directly probed not only with gravitational lensing observations (see Lapi & Cavaliere 2009b), but also in X rays as discussed below.

---

Send offprint requests to: lapi@roma2.infn.it

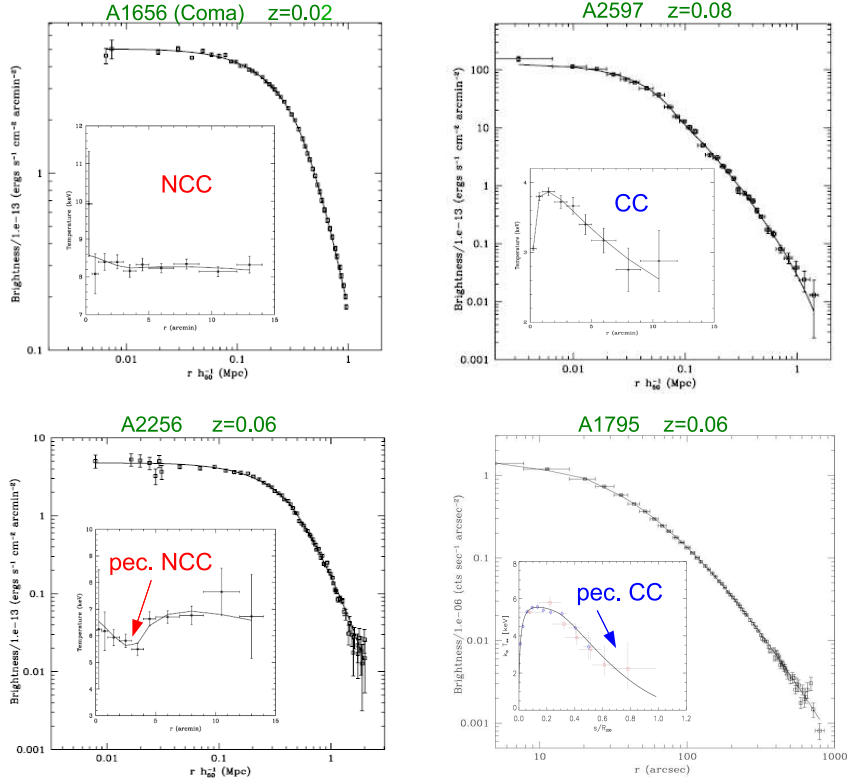


**Fig. 1.** The cluster Grand Design resulting from two-stage halo development and ICP analyses with the SM, is illustrated with examples of X-ray brightness profiles (projected temperatures in the insets) from Fusco-Femiano et al. (2009) and Lapi et al. (2010). Central entropy marks the CC/NCC dichotomy, while outer production modulates the outskirts.

## 2. An entropy primer

Secular accretion of intergalactic gas occurs along with DM's; the velocities are supersonic since the temperatures are as low as  $10^{-1}$  keV. Thus much entropy is generated at a radius  $r \approx R$  via accretion shocks which provide an effective bounding layer for the ICP (e.g., Lapi et al. 2005; Voit 2005). At the shock, gas inflowing with Mach number  $\mathcal{M} \gtrsim 2$  undergoes a temperature jump to  $T \propto \mathcal{M}^2$  and an enhancement of the number density  $n$  by a factor up to 4.

The ICP specific ‘entropy’  $k \equiv k_B T / n^{2/3}$  is correspondingly enhanced from intergalactic values of order  $10^2$  keV cm<sup>2</sup> by factors  $\mathcal{M}^2 / 4^{2/3} \sim 10$ . Moving toward the center, we expect the entropy to decrease to some  $10^1$  keV

cm<sup>2</sup> as the temperature  $k_B T \approx G m_p M(< r) / r$  goes up from  $R$  to  $r_{-2} = R/c$  by factors 2 – 5, while via adiabatic compression the density grows by several  $10^2$  to achieve equilibrium within the DM gravitational potential  $\Delta\phi$  as outlined by the classic isothermal  $\beta$ -model  $n \propto e^{\beta\Delta\phi}$ , see Cavaliere & Fusco-Femiano (1976).

With such an inferred baseline, we expect significant or even overwhelming central entropy injections from blastwaves launched by AGN outbursts (up to several  $10^1$  keV cm<sup>2</sup>, see Cavaliere et al. 2002; Valageas & Silk 1999; McNamara & Nulsen 2007), and even more by violent deep major mergers (up to several  $10^2$  keV cm<sup>2</sup>, see McCarthy et al. 2007; Markevitch & Vikhlinin 2007). On the other hand, radiative cooling in hydrostatic equilib-

rium (HE) can erode  $k_c$  over timescales  $t_c \approx 0.3 (k_c/15 \text{ keV cm}^2)^{1.2}$  Gyr. But AGNs recurring on similar scales may constitute an effective means to prevent a cooling catastrophe (e.g., Voit 2005; Vikhlinin et al. 2006).

### 3. Central classes and outer regions

To sharpen these estimates, we render the actual entropy run in the form

$$k(r) = k_c + (k_R - k_c) (r/R)^a, \quad (1)$$

consistent with recent analyses of wide cluster samples (Cavagnolo et al. 2009; Pratt et al. 2010); this embodies two *specific* parameters: the central level  $k_c$  and the outer slope  $a$ .

To compute in full the equilibrium of the ICP within the DM gravitational well, we base on our Supermodel (SM; see Cavaliere et al. 2009). An IDL algorithm to implement it may be found at <http://people.sissa.it/~lapi/supermodel/>.

#### 3.1. Cores, CC vs. NCC

From the latter we have found in CLFF09 that as  $k_c$  crosses a threshold around 20 keV cm<sup>2</sup> our temperature profiles *change* from a central drop typical of cool core (CC), to a plateau typical of non-cool core (NCC) clusters (see Molendi & Pizzolato 2001). We find that the latter feature a truly flat central brightness; in the temperatures some still bear the peculiar (if spherically averaged) imprint of a powerful, recently-driven blastwave that prevented or partially erased any cool core (see Fusco-Femiano et al. 2009; Rossetti & Molendi 2010). In addition, we have found that the NCCs are associated with low values of  $c \sim 3 - 5$ , and so by all accounts they must be *young*. CCs, on the other hand, generally feature higher concentrations  $c \sim 6 - 10$  and smoother profiles, so they look *older* in age, beyond the cosmic variance.

The resulting Grand Design for galaxy clusters is presented with specific examples in Fig. 1 and caption. Next we focus on the outer structure.

#### 3.2. Outskirts development

The slope  $a$  in Eq. (1) describes the powerlaw outward rise expected from the scale-free stratification of the entropy produced at the boundary shock as the cluster grows.

The slope  $a_R$  at  $r \approx R$  has been derived by CLFF09 from the standard shock boundary conditions and the adjoining HE maintained by thermal pressure, to obtain

$$a_R = 2.4 - 0.47 b_R. \quad (2)$$

Here  $b_R \equiv \mu m_p v_R^2 / k_B T_R$  marks the ratio of the potential to the thermal energy of the ICP (see Lapi et al. 2005; Voit 2005). This reads  $b_R \approx 3/2 \Delta\phi$  when a strong shock efficiently thermalizes into 3 degrees of freedom the in-fall energy; the latter is expressed in terms of the potential drop  $\Delta\phi$  experienced by successive shells of DM and gas that expand, and turn around at the radius  $R_{\text{ta}} \approx 2R$  to start their in-fall toward the shock located at  $R$ .

At any given cosmic time  $t$ , Eq. (2) holds at the current virial radius  $R(t)$ . On the other hand, the *specific* entropy deposited there is conserved during subsequent adiabatic compressions of the accreted gas into the DM gravitational well, while no other major sources or sinks of entropy occur down to central 10<sup>2</sup> kpc. So as the cluster outskirts develop out to the current  $R(t)$ , the inner entropy stratifies with a running slope  $a(r) = a_{R(t)}$  that retains its original values at the times of deposition.

Standard values  $a \approx 1$  (Tozzi & Norman 2001) are recovered on adopting the standard ratio  $R/R_{\text{ta}} \approx 0.5$ , and the potential drop  $\Delta\phi \approx 1 - (R/R_{\text{ta}}) \approx 0.5$  associated to a top-hat initial mass perturbation  $\delta M/M \propto M^{-1}$  that describes the collapse of the cluster *body* as a whole. From Eq. (2) this yields  $b_R \approx 2.7$  and  $a \approx 1.1$ . However, we expect variations of  $a(r)$  in the cluster outskirts.

#### 3.3. Expected entropy runs

This is because during the outskirts development the accretion rates  $\dot{M}/M \approx d/t \epsilon$  drop, due to two concurring space-time effects: (i) the cosmological slowdown of structure development at late cosmic *times*, described by

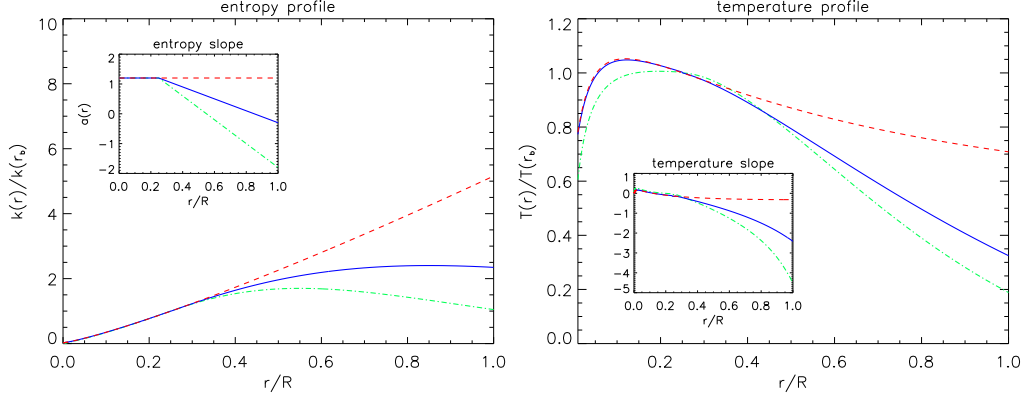


**Fig. 2.** Examples of entropy (left) and temperature (right) profiles computed with the SM: (red) dashed lines refer to Eq. (1) with  $k_c = 0$  and  $a = 1.2$ ; (blue) solid lines refer to Eq. (3) with  $k_c = 0$ ,  $a = 1.2$ ,  $r_b = 0.25R$ , and  $a' = 0.5$ ; (green) dot-dashed line refer to Eq. (3) with  $k_c = 0$ ,  $a = 1.2$ ,  $r_b = 0.25R$ , and  $a' = 1$ . The insets illustrate the corresponding logarithmic slopes. All profiles are normalized to the values at  $r = r_b$ .

values of  $d$  decreasing from  $2/3$  to  $1/2$  (see Weinberg 2008); (ii) the *spatial* shape of the initial perturbations  $\delta M/M \propto M^{-\epsilon}$  as described by the parameter  $\epsilon$  taking on values  $> 1$  in perturbation wings that scarcely feed the outskirts growth. The latter effect may be offset (and represented with a smaller effective  $\epsilon$ ) in biased environments, dense or adjacent to filamentary large-scale structures.

In average environs where  $\epsilon > 1$  applies, the potential drop is shallower relative to the body value and reads  $\Delta\phi = [1 - (R/R_{\text{ta}})^{3\epsilon-2}]/(3\epsilon-2)$ , so leading to larger values of  $r_b$  and *lower* values of  $a$ . Thus for  $r$  increasing towards the outskirts we expect the entropy profiles to deviate more and more downward from a simple powerlaw, see Fig. 2.

The decline of  $a$  from the body value will begin from a radius  $r_b \sim r_{-2}$  where matter stratified just after the transition time  $z_t$  at the beginning of the outskirts growth. Such a radius is estimated in terms of the present concentration and radius  $R$  in the form  $r_b/R \approx r_{-2}/R = 1/c$  that takes on values around 0.2 for a typical concentration  $c \approx 6$  of CC clusters.

Thus under the *lower* accretion rates prevailing at *later* times in average environs, we expect the entropy slope  $a(r)$  to decline to-

ward smaller or even negative values; the corresponding entropy run will *flatten* out or even turn down into the cluster outskirts. This will imply a sharp *decline* of the outer temperatures  $T(r) \propto k(r)n^{2/3}(r)$ , as the overall density decline is insufficiently offset or is even reinforced by the entropy run.

#### 4. A case study from current data

The above entropy behavior may be expressed in terms of a simple parametric form: a constant slope  $a$  applying in the cluster body for  $r \leq r_b$  to produce an inner shape like that in Eq. (1); a decline (e.g., a linear one) for  $r > r_b$  with slope  $a' \equiv (a - a_R)/(R/r_b - 1)$  toward the outer value  $a_R < a$  at  $r = R$ , to produce the outer shape (see Fig. 2)

$$k(r) = k_R (r/R)^{a+a'} e^{a'(R-r)/r_b} . \quad (3)$$

The ensuing temperature profiles provided by the SM are illustrated in Fig. 2. This shows that a flattening or even decreasing entropy run as in Eq. (3) produces in the cluster outskirts peculiarly *steep* temperature profiles. Next we focus on two clusters where temperature data have been recently obtained out to  $r \approx R$ ; the uncertainties are quoted at the 68% level.

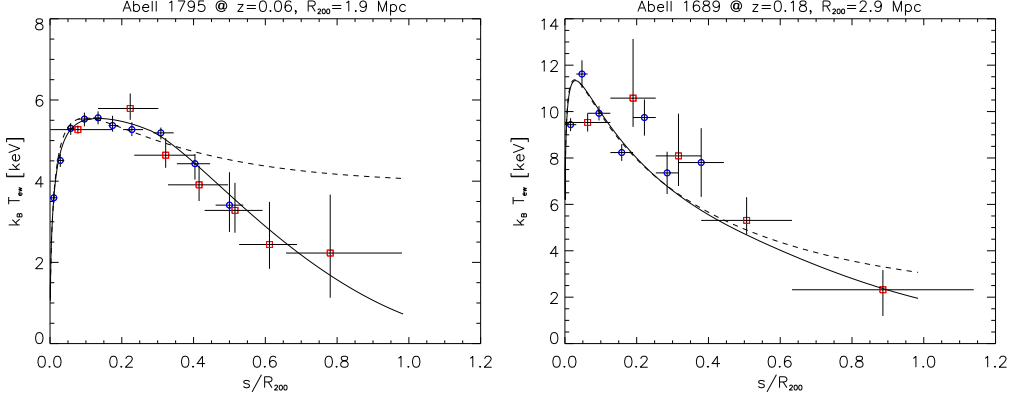


**Fig. 3.** Profiles of projected X-ray temperature for the CC clusters A1795 (left) and A1689 (right). Data from XMM-Newton (blue circles) and Suzaku (red squares), see refs. in the text. Our best-fits from the SM based on Eq. (3) are illustrated by the solid lines, while dashed lines refer to the fits based on Eq. (1). Temperature profiles with intermediate steepness hold for the CC clusters PKS0745-191 at  $z \approx 0.1$  and A2204 at  $z \approx 0.15$  (see Lapi et al. 2010).

For the CC cluster A1795 at  $z = 0.063$ , in Fig. 3 (left panel) we overplot on the temperature data from XMM-Newton and Suzaku (Snowden et al. 2008; Bautz et al. 2009) the best-fit (solid line) from the SM with the entropy profile in Eq. (3). The parameters read:  $k_c < 10 \text{ keV cm}^2$ ,  $a = 1.2^{+0.3}_{-0.3}$ ,  $r_b/R = 0.28^{+0.02}_{-0.02}$ , and  $a' = 1.8^{+1.3}_{-1.3}$ , with a good value of the reduced  $\chi^2 = 0.3$ . We also evaluate the concentration  $c = 8.5^{+1.9}_{-1.9}$ . The simple entropy profile of Eq. (1) with  $a' = 0$  would result in a worse best-fit (dashed line) with  $\chi^2 = 2.6$ .

As to the cluster A1689 at  $z = 0.1832$ , this is often classified as a CC although the temperature inner drop from its high peak is controversial to some extent (see Riemer-Sørensen et al. 2009). In Fig. 3 (right panel) we overplot on the temperature data averaged over 4 sectors from XMM-Newton and Suzaku (see Snowden et al. 2008; Kawaharada et al. 2010) the best-fit (solid line) from the SM with the entropy profile in Eq. (3). The parameters read:  $k_c < 10 \text{ keV cm}^2$ ,  $a = 0.7^{+0.3}_{-0.3}$ ,  $r_b/R = 0.5^{+0.1}_{-0.1}$ , and  $a' = 1.6^{+1.2}_{-1.2}$ , with an acceptable values of the reduced  $\chi^2 = 1.5$ . We also estimate the concentration  $c = 12.4^{+5.3}_{-5.3}$ , consistent with gravitational lensing observations (see Broadhurst et al. 2008; Lapi & Cavaliere 2009b). The sim-

ple entropy profile of Eq. (1) with  $a' = 0$  would result in a best-fit (dashed line) with  $\chi^2 = 1.7$ .

We have also computed the related brightness profiles, finding non-monotonic outer slopes; these first flatten where the entropy begins to deviate from a powerlaw, and then steepen where the entropy turns down. Such detailed features go beyond the resolution and/or the background-limited sensitivity of current instruments, but will be widely observed and easily pinpointed with WFXT (see <http://wfxt.pha.jhu.edu/>).

## 5. Summary and perspectives

These data support the view that outer entropy production is reduced especially at low  $z_{\text{obs}}$ , as the inflows of DM and intergalactic gas peter out. This view stems from two concurring sources: (i) the *cosmological* slowdown in the growth of outskirts developing at late cosmic times; (ii) shallow perturbation wings scantily feeding the outskirts growth in average or poor environs.

Under such conditions, we expect the entropy profile to progressively flatten out or even decrease into the cluster outskirts as represented by Eq. (3). Whence the SM from

entropy-modulated equilibrium of the ICP and strong boundary shocks leads to envisage specifically steep outer temperatures.

On the other hand, we expect the accretion rates to be sustained in rich environs, or in cluster sectors adjacent to filamentary large-scale structures; shallower temperature runs are likely to prevail there. These can be effectively probed with a pointing instrument of high spectral sensitivity and resolution like IXO (see <http://ixo.gsfc.nasa.gov/>).

But from an adjacent filament blobs of DM and cold gas can easily fall into the cluster, leading to cold dense spots that may enforce a local breakdown of HE. The latter will fail anyway beyond  $R$  together with the DM equilibrium. In addition, as  $\dot{M}$  decreases to the point that the infall velocities go down to transonic values, the shocks weaken, thermalization becomes inefficient (see CLFF09), the entropy production is terminated, and thermal pressure cannot support HE any longer.

To sum up, even on assuming standard boundary shocks with optimal energy conversion and HE, we find temperature profiles declining sharply outwards. We propose these to stem from progressive *exhaustion* of mass inflow, especially for young clusters in average or poor environments at lower  $z_{\text{obs}}$ ; such a trend is consistent with that looming out at decreasing redshifts for the clusters in Fig. 3 and caption. Conversely, at higher  $z_{\text{obs}}$  we expect sustained accretion, but also more frequent cold dense clumps infalling and departing from HE.

To conclude, we stress that with  $\dot{M}$  decreasing rich astrophysics is likely to set in at the *interface* between the ICP and the intergalactic medium, including hydrodynamics in conditions of long mean free paths and slow/incomplete bulk motion conversion. As indicated above, such phenomena call for extensive probing even at  $z \gtrsim 0.2$  with the next generation of X-ray telescopes planned to detect and resolve low-surface brightness features of the intracluster plasma (see Giacconi et al. 2009), like WFXT and IXO.

*Acknowledgements.* The material presented here is based upon the paper by Lapi et al. (2010).

## References

- Bautz, M.W., et al. 2009, PASJ, 61, 1117  
 Broadhurst, T., et al. 2008, ApJ, 685, L9  
 Cavagnolo, K. W., et al. 2009, ApJS, 182, 12  
 Cavaliere, A., Lapi, A., and Fusco-Femiano, R. 2009, ApJ, 698, 580 [CLFF09]  
 Cavaliere, A., Lapi, A., and Menci, N. 2002, ApJ, 581, L1  
 Cavaliere, A., and Fusco-Femiano, R. 1976, A&A, 49, 137  
 Diemand, J., Kuhlen, M., and Madau, P. 2007, ApJ, 667, 859  
 Fusco-Femiano, R., Cavaliere, A., and Lapi, A. 2009, ApJ, 705, 1019  
 George, M.R., et al. 2009, MNRAS, 395, 657  
 Giacconi, R., et al. 2009, in Astro2010: The Astronomy and Astrophysics Decadal Survey, Science White Papers, no. 90  
 Kawaharada, M., et al. 2010, ApJ, 714, 423  
 Lapi, A., Cavaliere, A., and Fusco-Femiano, R. 2010, A&A, 516, A34  
 Lapi, A., and Cavaliere, A. 2009a, ApJ, 692, 174  
 ——— 2009b, ApJ, 695, L125  
 Lapi, A., Cavaliere, A., and Menci, N. 2005, ApJ, 619, 60  
 Leccardi, A., and Molendi, S. 2008, A&A, 486, 359  
 Markevitch, M., and Vikhlinin, A. 2007, Phys. Rep., 443, 1  
 McCarthy, I.G., et al. 2007, MNRAS, 376, 497  
 McNamara, B.R., and Nulsen, P.E.J. 2007, ARA&A, 45, 117  
 Molendi, S., and Pizzolato, F. 2001, ApJ, 560, 194  
 Navarro, J.F., et al. 2010, MNRAS, 402, 21  
 Pratt, G.W., et al. 2010, A&A, 511, 85  
 Riemer-Sørensen, S., et al. 2009, ApJ, 693, 1570  
 Rossetti, M., and Molendi, S. 2010, A&A, 510, 83  
 Snowden, S.L., et al. 2008, A&A, 478, 615  
 Tozzi, P., and Norman, C. 2001, ApJ, 546, 63  
 Valageas, P., and Silk, J. 1999, A&A, 350, 725  
 Vikhlinin, A., et al. 2006, ApJ, 640, 691  
 Voit, G. M. 2005, Rev. Mod. Phys., 77, 207  
 Weinberg, S. 2008, Cosmology (Oxford: Oxford Univ. Press)  
 Zhao, D.H., et al. 2003, MNRAS, 339, 12